


 Cite this: *RSC Adv.*, 2021, 11, 38033

# Application of high-efficiency green fluorescent carbon dots prepared by acid catalysis in multicolour LEDs

 Yulong An,<sup>a</sup> Can Liu,<sup>ab</sup> Yan Li,<sup>a</sup> Menglin Chen,<sup>a</sup> Yunwu Zheng,<sup>ab</sup> Hao Tian,<sup>c</sup> Rui Shi,<sup>a</sup> Xiahong He<sup>\*a</sup> and Xu Lin<sup>id\*ab</sup>

Acidic reagents play an important role in the preparation of carbon dots (CDs). Therefore, we prepared efficient green fluorescent CDs by potassium bisulfate, acetic acid and hydrochloric acid catalysis and discussed why the acid catalyst induced a fluorescence redshift and improved the quantum yield of the CDs. Furthermore, the concentration-dependent photoluminescence behaviour of the CDs was characterized. CD/PVA composites emitting green to yellow light were obtained by exploiting the fluorescence tunability of CDs. Based on different light-emitting diode substrates, green, yellow and white light-emitting diodes with excellent performance were prepared.

 Received 30th September 2021  
 Accepted 18th November 2021

DOI: 10.1039/d1ra07280c

[rsc.li/rsc-advances](http://rsc.li/rsc-advances)

## Introduction

Since the first discovery of carbon dots (CDs) in 2004, which represented a new breakthrough in the field of carbon nanomaterials, research on fluorescent CDs has attracted increasing attention from scientists.<sup>1</sup> Due to their advantages of a simple preparation method, low toxicity, good photostability and high biocompatibility, CDs are widely used in sensing, biological imaging, catalysis and lighting.<sup>2,3</sup> Generally, the preparation of CDs is divided into top-down and bottom-up approaches, and the solvothermal method, which includes the polymerization, dehydration and carbonization of carbon sources, is the most widely used bottom-up synthesis method.<sup>4–7</sup> Furthermore, acid catalysis has been shown to be beneficial for the hydrolysis and carbonization of carbon sources and to influence the photoluminescence of CDs.<sup>8–10</sup> Acidic reagents can increase the abundance of electron absorbing groups on the surface of prepared CDs, increase the size of the particles, and redshift the photoluminescence wavelength,<sup>11,12</sup> which are significant for the design and synthesis of polychromatic fluorescent CDs. Wang *et al.*<sup>11</sup> produced a series of CDs through a scalable acidic reagent engineering strategy. Full-colour polymer luminescent films and various white light-emitting diodes

(LEDs) with high colour rendering indices were synthesized by mixing various CDs in appropriate proportions, which promoted the progress of carbon-based luminescent materials in the preparation of promising films and devices.

In many fields, CDs are used as down-conversion phosphors for the preparation of white LEDs, and they have received extensive attention.<sup>13–16</sup> To optimize the properties of CDs, much effort has been devoted to improving their potential applications in white LEDs. A combination of a blue or ultraviolet (UV) LED chip and multicolour fluorescent CDs is commonly used to produce white light.<sup>17–19</sup> In a blue-pumped white LED, the blue light emitted by the chip is used as the excitation light source for the CDs and participates in light mixing as part of the white light spectrum, which reduces the use of phosphors and the cost. A reduction in the number of light conversions can also reduce light loss, thus improving the efficiency of white LEDs.<sup>20,21</sup>

In this study, we investigated the effects of three commonly used acids as catalysts and *m*-phenylenediamine as a carbon source on fluorescent CDs. The structures, chemical groups and optical properties of the resulting CDs were characterized and analysed, and the effects of different acid catalysts on the fluorescence and functional group structure of the CDs were studied. The fluorescence of the CDs was tuned by adjusting the concentration of the CDs solution, and a wide spectral fluorescence response range from green to yellow was observed. On this basis, polychromatic CDs polystyrene (PVA) films were prepared and successfully applied to colour LEDs. Green and yellow fluorescent LEDs were prepared by covering 365 nm luminescent ultraviolet LED chips with the CDs/PVA composites, and white fluorescent LEDs were prepared by covering 460 nm luminescent blue LED (B-LED) chips with yellow films.

<sup>a</sup>Key Laboratory for Forest Resources Conservation and Utilization in the Southwest Mountains of China, Southwest Forestry University, Kunming, China. E-mail: [linxunefu@126.com](mailto:linxunefu@126.com)

<sup>b</sup>Key Laboratory of State Forestry Administration for Highly-Efficient Utilization of Forestry Biomass Resources in Southwest China, Southwest Forestry University, Kunming, China

<sup>c</sup>Agro-products Processing Research Institute, Yunnan Academy of Agricultural Sciences, Kunming, China



## Materials and methods

### Materials

Column chromatography was performed using 200–300 mesh silica gel. *m*-Phenylenediamine (99.0%), ethanol (99.7%), potassium bisulphate (99.0%), acetic acid (99.5%), hydrochloric acid (38.0%), dichloromethane (99.0%) were provided by Shanghai Titan Scientific Co., Ltd (Shanghai, China). All reagents were used as received without further purification unless otherwise specified. Deionized (DI) water was used throughout this study.

### Methods

Transmission electron microscopy (TEM) images was carried out using a FEI Tecani G2 F20 operating at an acceleration voltage of 200 kV. UV-vis spectra were recorded with a Shimadzu UV-2600 spectrometer. Fluorescence measurements were collected using a Shimadzu fluorescence spectrophotometer RF-6000. Nanosecond fluorescence lifetime experiments were performed by the time correlated single-photon counting (TCSPC) system (HORIBA Scientific iHR 320). A 290 nm (<1 ns) and a 485 nm (<200 ps) nano-LED light source were used to excite the samples. CIE chromaticity coordinate was measured by KONICA MINOLTA CS-150 colorimeter. The Fourier transform infrared (FT-IR) spectra were obtained in transmission mode on a Thermo Scientific Nicolet iS5 spectrometer (Waltham, MA, USA) with the KBr pellet technique, and 8 scans at a resolution of 1 cm<sup>-1</sup> were accumulated to obtain one spectrum. X-ray photoelectron spectroscopy (XPS) was investigated by using K-Alpha spectrometer with a mono X-ray source Al K $\alpha$  excitation (1486.6 eV). Binding energy calibration was based on C 1s at 284.8 eV.

### Quantum yield measurements

QYs of the obtained three CDs were determined by a relative method. The CDs ethanol solution was placed in a colorimetric dish to determine its QY, and the solvent ethanol was used as a blank sample for reference determination. Rhodamine 6G (QY = 95% in ethanol) was chosen as a reference, with an emission range of 480–560 nm.

The QY of a sample was then calculated according to the following equation:

$$\Phi = \Phi_R(A_R/A)(II/I_R)(n^2/n_R^2)$$

where  $\Phi$  is the QY of the testing sample,  $I$  is the testing sample's integrated emission intensity,  $n$  is the refractive index (1.36 for ethanol), and  $A$  is the optical density. The subscript "R" refers to the referenced fluorescence dyes of known QYs. Adjust the concentrations of the CDs and reference fluorescent dye solutions so that the optical absorbance values were between 0 to 0.1 at 365 nm.

### Synthesis of CDs

*m*-Phenylenediamine as precursor and acid reagent as auxiliaries, CDs was synthesized by solvothermal method. Potassium bisulfite (0.1 g) was added to 10 mL ethanol containing *m*-phenylenediamine (0.5 g) under intense stirring, then transferred to a polytetrafluoroethylene (PTFE) lined autoclave and heated at 180 °C for

12 hours. Cool naturally to room temperature to obtain a dark green solution. The preparation process of the other two CDs is the same as above, except that potassium bisulfite is changed into acetic acid (1.0 mL) and concentrated hydrochloric acid (0.5 mL) to obtain the other two green fluorescent suspensions. After the pH value of the suspensions is adjusted to 7, the three CDs solutions were dried by rotary evaporation in vacuum, then redissolved with dichloromethane, and then purified by silica gel column chromatography with a mixture of dichloromethane and ethanol as eluent (dichloromethane : ethanol = 9 : 1). This process is repeated three times to remove excess impurities and unreacted precursors. After solvent removal and further vacuum drying, three kinds of CDs were obtained with a yield of 10–20 wt%.

### Preparation of polychromatic CDs-1/PVA films

Green to yellow-orange fluorescent CDs-1/PVA thin films were prepared by a simple method. Dissolve 1.0 mg, 5.0 mg, 10.0 mg and 20.0 mg CDs in 2.0 mL PVA aqueous solution (5% by weight), stir to fully dissolve the CDs, and ultrasonic continued to form a uniformly dispersed solution. Pour CDs-1/PVA solution into a glass mold and dry it in a confined space at room temperature for 12 h. Four CDs-1/PVA films with different fluorescence colors were obtained.

### Fabrication of LEDs

The emission peaks of UV-LEDs and B-LEDs chips are located at 365 nm and 420 nm, and the operating voltage is 3.0 V. 5.0 mg and 50 mg CDs samples were mixed with 5.0 mL poly (vinyl alcohol) (PVA) aqueous solution (5% by weight) respectively. After stirring evenly, the resulting mixture solution was applied to the UV-LED chip with 2 to 4 drops. The LED chips containing CDs/PVA composite fluorescent matrix were then dried at room temperature for 24 h. As a result, green and yellow fluorescent LEDs were achieved. A white fluorescent LED was prepared on a B-LED chip by mixing 50 mg CDs with a PVA solution with a total volume of 5.0 mL.

## Results and discussion

High-efficiency green fluorescent CDs were prepared by a solvothermal method with *m*-phenylenediamine as the raw material under acidic conditions. Three common acids, potassium bisulfate (weak inorganic acid), acetic acid (organic acid) and hydrochloric acid (strong inorganic acid), were selected as catalysts for CDs synthesis. For simplicity, the CDs prepared in the above three acidic reagents were labelled CDs-1, CDs-2 and CDs-3. For comparison, the blue fluorescent CDs synthesized with *m*-phenylenediamine as the raw material under neutral conditions were named CDs-0.<sup>22</sup> The obtained CDs exhibited good solubility in water, ethanol, chloroform and other common solvents and could be dispersed in ethanol to form a fluorescent solution (Fig. 1), which glowed bright green under ultraviolet light.

### Optical characteristics and structure

The UV/Vis absorption spectra of the CDs were measured in ethanol, as shown in Fig. 2. In the high-energy absorption



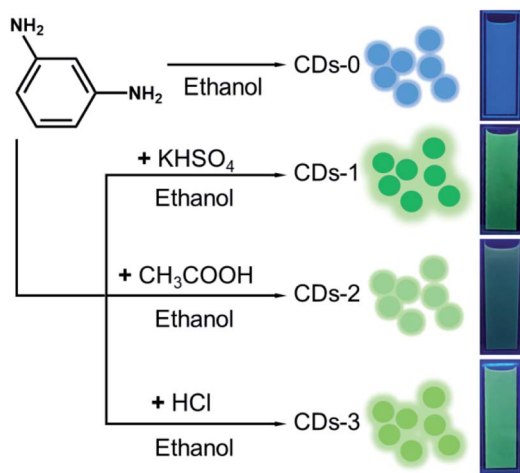


Fig. 1 Schematic illustration of the preparation of four CDs. Right: four kinds of CDs dispersed in ethanol under ultraviolet light at 365 nm.

region, all four CDs exhibited strong absorption. The absorption peaks at 200–280 nm were attributed to the eigenstate ( $\pi-\pi^*$ ) transition in the aromatic domain (C=C).<sup>23</sup> The absorption peaks at 280–350 nm were assigned to the C=O eigenstate ( $n-\pi^*$ ) transition.<sup>24</sup> Compared with that of CDs-0, the absorption peaks of CDs treated with acid were significantly redshifted, especially those of CDs-1 and CDs-3. In the low-energy region, the absorption peaks of the three CDs treated with acid appear between 420 and 520 nm because of the surface defect state of the CDs. The absorption peak between 420 and 520 nm is attributed to the defect state transition caused by surface functional groups, which may be due to the catalytic action of acid, so that a large number of functional groups adhere to the surface of CDs.<sup>24</sup> These groups may be amine groups, hydroxyl groups or other oxygen-containing functional groups on the CDs surface, resulting in samples with a surface state different from that of CDs-0. In addition, CDs-1 and CDs-3 gave rise to obvious broad absorption peaks in the low-energy region compared with CDs-2.

Fig. 3b–d shows the fluorescence emission (PL) spectra of three kinds of CDs recorded in ethanol solution. The emission peaks of CDs 1–3 were observed at 502, 500, and 513 nm, respectively. The emission centre remained almost the same as

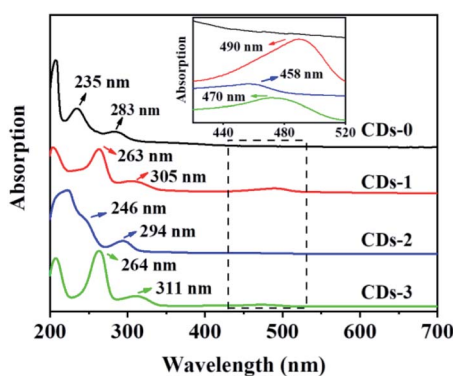


Fig. 2 Absorption spectra of CDs-0, CDs-1, CDs-2 and CDs-3 in ethanol. The inset is the enlarged absorption spectra ( $c = 0.1 \text{ mg mL}^{-1}$ ).

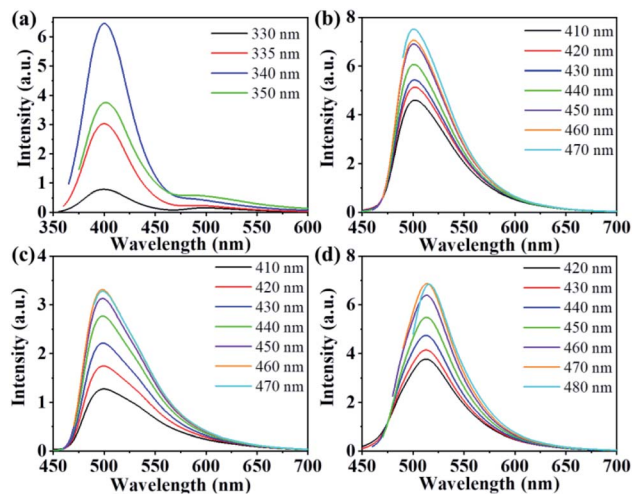


Fig. 3 (a) Fluorescence spectra of CDs-0 in ethanol at different excitation wavelengths; (b–d) fluorescence spectra of CDs-1, CDs-2 and CDs-3 in ethanol at different excitation wavelengths ( $c = 0.1 \text{ mg mL}^{-1}$ ).

the excitation signal increased, showing an excitation-independent characteristic. Compared with that of CDs-0 (Fig. 3a), the maximum emission peaks of CDs 1–3 changed from 400 to 500 nm, and the fluorescence colour changed from blue to bright green. In addition, the quantum yield of CDs-0 was 4.8%,<sup>22</sup> and the quantum yields of CDs 1–3 were 46.2%, 14.6% and 36.4%, respectively. These results show that the preparation of CDs with an acid catalyst can not only cause a redshift in the fluorescence spectrum but also significantly improve the fluorescence quantum yield of the CDs. In particular, the quantum yield of CDs-1 was as high as 46.23%. Compared with CDs-2 and CDs-3, CDs-1 has better fluorescence, nearly ten times higher than the optical performance of 4.8% observed for CDs-0.

The morphology of the prepared samples was examined by transmission electron microscopy (TEM). Representative TEM images of CDs-1, CDs-2 and CDs-3 are shown in Fig. 4a–c,

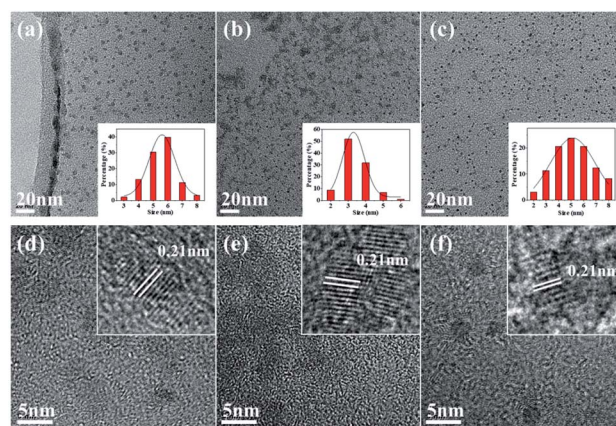


Fig. 4 (a–c) TEM images of CDs-1, CDs-2 and CDs-3. Illustration: histogram and Gaussian curve of the particle size distribution of CDs-1, CDs-2 and CDs-3; (d–f) HR-TEM images.



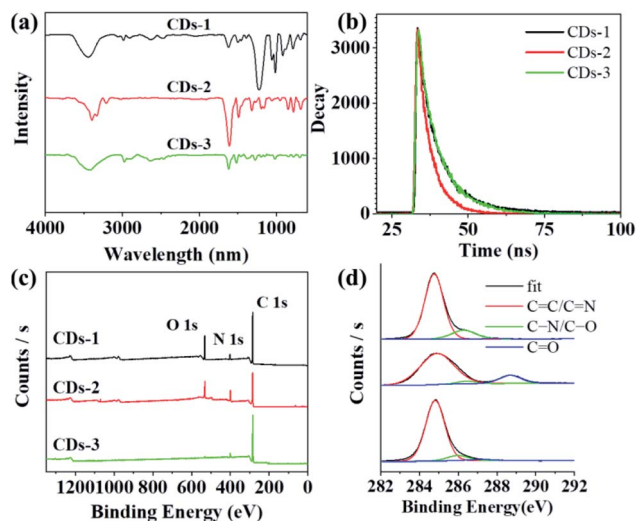


Fig. 5 (a) FT-IR spectra of CDs-1, CDs-2 and CDs-3; (b) photoluminescence lifetime attenuation patterns of CDs-1, CDs-2 and CDs-3 in ethanol ( $c = 0.1 \text{ mg mL}^{-1}$ ) ( $\lambda_{\text{ex}} = 500 \text{ nm}$ ); (c) XPS spectra of CDs-1, CDs-2 and CDs-3; and (d) high-resolution C 1s spectra of different CDs.

respectively. We can clearly see the uniform spherical particle-type morphology of these samples, and they show good monodispersity. The average particle sizes of CDs-1 to CDs-3 were 5.5 nm, 3.4 nm and 5.2 nm, respectively. Similar to the fluorescence of the CDs, the particle size of the CDs was found to be proportional to the fluorescence yield, indicating that the quantum size effect has a certain influence on the fluorescence properties of the CDs. Fig. 4d–f shows HRTEM images of CDs-1 to CDs-3, showing a well-resolved lattice spacing of 0.21 nm, close to the (100) diffraction phase of the crystal plane to graphite carbon, which indicates that well-crystallized CDs have been successfully synthesized.<sup>25</sup>

The Fourier transform infrared (FTIR) spectrum shown in Fig. 5a shows that the surface of all CDs samples is rich in polar functional groups, such as O–H/N–H (peaks at  $3400 \text{ cm}^{-1}$ ), C=O (peaks at  $1620 \text{ cm}^{-1}$ ) and C–O (peaks at  $1050 \text{ cm}^{-1}$ ), thus ensuring the excellent solubility of these CDs in polar solutions.<sup>26</sup> In addition, tensile vibrations of the C=O ( $1620 \text{ cm}^{-1}$ ) and C=N ( $1500 \text{ cm}^{-1}$ ) bonds were observed for each sample, indicating that a polyaromatic structure was formed in the CDs during the reaction.<sup>27,28</sup> It is worth noting that CDs-2 shows a very strong carbonyl signal peak, which may have a negative impact on the fluorescence performance.<sup>4</sup> In addition, significant differences in fluorescence emission mechanisms were identified by measuring the fluorescence lifetimes (Fig. 5b). The fluorescence lifetimes of CDs-1, CDs-2 and CDs-3 were determined to be 4.92, 3.74, and 4.82 ns, respectively. The fluorescence lifetime of CDs-2 was much shorter than those of CDs-1 and CDs-3.

X-Ray photoelectron spectroscopy (XPS) was used to further investigate the surfaces of these samples. The full spectra presented in Fig. 5c show three typical peaks: C 1s (285 eV), N 1s (400 eV), and O 1s (531 eV).<sup>29</sup> These findings indicate that the samples consisted of the same elements. CDs-2 has the lowest

content of C element, which may not be conducive to the formation of conjugated structure. In the high-resolution spectra (Fig. 5d), the C 1s band can be decomposed into three peaks, corresponding to the C=C/C=N bond (284.8 eV), the C–N/C–O bond (286.3 eV) and the C=O bond (288.2 eV).<sup>30</sup> The higher C=C/C=N ratios of CDs-1 and CDs-3 indicating the formation of more  $\text{sp}^2$  carbon domain in CDs, which may lead to higher fluorescence efficiency (Table 1).<sup>4</sup>

### Concentration-dependent wide spectral range response

Surprisingly, in addition to the fluorescence redshift and the QY improvements, acid-catalysed CDs exhibit a concentration-dependent redshift in the fluorescence.<sup>31</sup> As shown in Fig. 6a, a series of CDs with different concentrations were prepared in ethanol ( $c = 0.1, 1.0, 2.0, 5.0, 10.0, 20.0 \text{ mg mL}^{-1}$ ) for direct observation. With increasing CDs concentration, the colour of the solution changes from almost transparent to dark green in the sun. In addition, upon excitation with 365 nm ultraviolet light, the CDs in ethanol showed concentration-regulated fluorescence. With increasing concentration, the fluorescence of the CDs changed from green to yellow (Fig. 6b). Normalized photoluminescence spectra of the CDs were obtained by fluorescence detection of CDs-1 solutions with six different concentrations. The photoluminescence peaks were observed at approximately 502, 511, 524, 540, 552 and 575 nm (Fig. 6d), showing a wide spectral response characteristic similar to that of panchromatic CDs. Upon adjusting the CDs concentration, the photoluminescence peaks varied in the range of 502–575 nm, and the fluorescence colour ranged from green to yellow. Increasing the CDs concentration promoted the aggregation of CDs and led to cross-linking and a fluorescence redshift, and no fluorescence self-quenching occurred. To investigate the mechanism of the concentration-dependent fluorescence redshift of the CDs, the UV absorption spectra of CDs solutions with six different CDs concentrations were measured. As mentioned above, the whole absorption spectrum can be divided into three bands, at 263, 305 and 490 nm (Fig. 6c). As the concentration increased, the value of  $I_{490}/I_{263}$  increased from 0.11 to 0.35, indicating that the absorption ratio of the surface state increased significantly.<sup>32</sup> It can be seen from the above results that the aggregation of CDs leads to an increasing interaction of surface states between the CDs and the redshift of the fluorescence.

Table 1 Elemental proportions and chemical bonds in CDs-1, CDs-2 and CDs-3

	CDs-1 (%)	CDs-2 (%)	CDs-3 (%)
C 1s	76.3	64.3	92.4
O 1s	5.3	12.4	5.5
N 1s	18.4	23.3	2.1
C=C/C=N	88.0	75.0	85.0
C–N/C–O	11.0	6.0	14.0
C=O	1.0	19.0	1.0



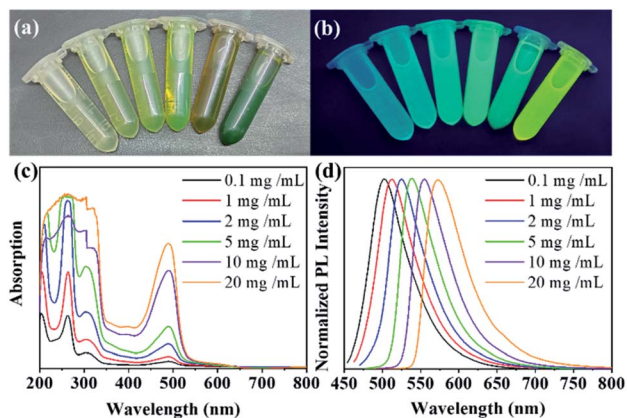


Fig. 6 Optical images of different concentrations of CD-1 in ethanol under natural light (a) and ultraviolet light (b) (from left to right,  $c = 0.1, 1.0, 2.0, 5.0, 10.0, 20.0$  mg mL<sup>-1</sup>), (c) UV/Vis absorption spectra and (d) fluorescence spectra.

### Colourful fluorescent CD/PVA film

By exploiting the adjustable fluorescence characteristics at different concentrations, we prepared green to yellow luminescent CD/PVA composite films by adjusting the concentration of CD-1 in PVA in solution. It can be seen from the photographs (Fig. 7a and b) that by adjusting the concentration of CD-1 in PVA, a green to yellow luminescent CD/PVA composite film was obtained, consistent with the fluorescence behaviour in the solution. As shown in Fig. 7c–f, the fluorescence spectrum shows fluorescence emission peaks of the CD/PVA composite film at 500, 512, 527 and 550 nm as the concentration of CD-1 in the film increased from low to high. The redshift of the fluorescence induced by the aggregation of CD-1 in the PVA films shows that CD-1 has great application potential in the preparation of colour fluorescent films.

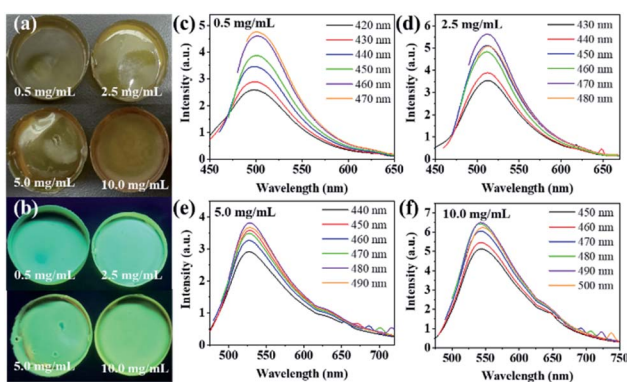


Fig. 7 Image of a CD's fluorescent film under visible light (a) and ultraviolet light (b) at 365 nm; (c–f) fluorescence spectra of the film (corresponding to the film optical images from left to right and top to bottom).

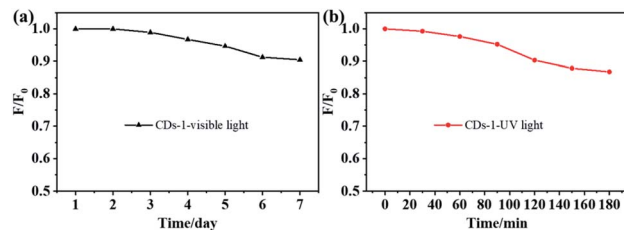


Fig. 8 Decay curve of FL intensity of CD-1 with increasing visible light (a) and UV light (b) time.

### Multicolour LED

In order to explore the stability of the fluorescence of CD-1, we studied its spectral changes in different visible and ultraviolet light continuous irradiation time. The maximum attenuation rate of the fluorescence intensity of the CD-1 under visible light for 7 days is less than 10% (Fig. 8a). Meanwhile, the attenuation rate of the fluorescence intensity of the CD-1 is less than 15% after 3 hours of continuous ultraviolet light ( $\lambda = 365$  nm) (Fig. 8b).

Based on the fluorescence stability of CD-1 and its unique excitation behaviour in solid polymer matrix, the prepared CD-1 can be used as light-emitting diode material. To verify that CD-1 is excited by a UV-LED chip as a phosphor, we prepared green fluorescent and yellow fluorescent LEDs by coating CD-1/PVA composites with different concentrations of CD-1 on a UV-LED chip (365 nm excitation). The fluorescence photographs and EL spectra are shown in Fig. 9a and c. The maximum emission peak of the green LED is 500 nm, while the wide emission peak of the yellow LED is concentrated at 550 nm. Therefore, we can use the yellow fluorescence behaviour of CD-1 at high concentrations to prepare white LEDs by combining CD-1/PVA composites with a blue LED chip (B-LED, 460 nm excitation). The B-LED emits blue light after the power is turned

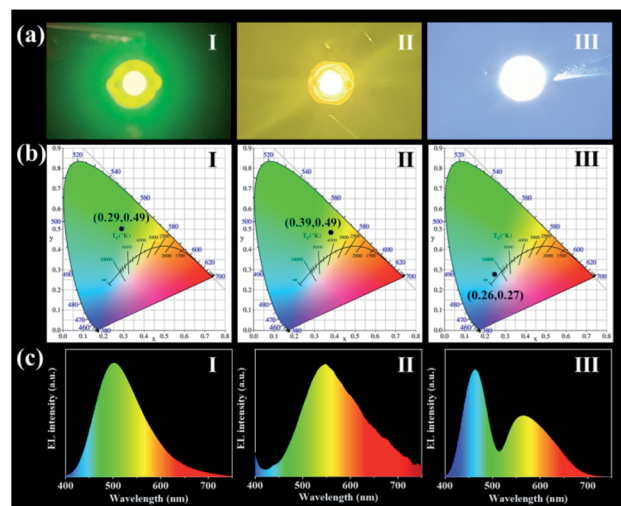


Fig. 9 (a) Photoluminescence photograph (I–III); (b) CIE chromaticity coordinates (I–III); and (c) PL emission spectra (I–III) of green, yellow and white LEDs.



on, and some of the blue light is absorbed by CDs-1 and converted into yellow light.<sup>33–35</sup> Another portion of the blue light passes through the CDs-1/PVA composite and mixes with yellow light to form white light. Fig. 9c(III) shows the emission spectrum of the white LED. The emission peaks near 460 nm and 550 nm were attributed to the B-LED chip and CD-1/PVA composite, respectively. As shown in Fig. 9b, the CIE coordinates of the green, yellow and white LEDs are (0.22, 0.41), (0.38, 0.47) and (0.50, 0.43). The above results show the potential application of acid-catalysed CDs in the field of LEDs.

## Conclusions

In conclusion, efficient green fluorescent CDs were synthesized by a solvothermal method with *m*-phenylenediamine as the raw material and acid as the catalyst. Under the catalysis of an acidic reagent, the fluorescence of CDs prepared by *m*-phenylenediamine changed from blue to green, accompanied by a significant increase in the quantum yield. The fluorescence of CDs-1 prepared with potassium bisulfate was the best, with a quantum yield of 46.2%. In addition, by adjusting the concentration of CDs-1 solution and enhancing the interaction of the CDs surface states, the fluorescence of CDs-1 could be tuned from green to yellow without fluorescence self-quenching. Using this fluorescence characteristic, a series of colour CDs-1/PVA composites were prepared with fluorescence from green to yellow. In addition, green and yellow fluorescent LEDs were prepared by coating the CDs-1/PVA composites on UV-LED chips, while white fluorescent LEDs were prepared by coating yellow fluorescent CDs-1/PVA composites on B-LED chips. This study provides a new method for the development of efficient green fluorescent CDs, which have excellent application potential in optoelectronic devices.

## Author contributions

Conceptualization, Y. A. and C. L.; methodology, Y. A. and X. L.; writing – original draft preparation, Y. A.; writing – review and editing, Y. L., M. C. and Y. Z.; visualization, R. S.; supervision, H. T.; project administration, X. H.; funding acquisition, X. L. All authors have read and agreed to the published version of the manuscript.

## Conflicts of interest

The authors declare that the research was conducted in the absence of any commercial or financial relationships that could be construed as a potential conflict of interest. There are no conflicts to declare.

## Acknowledgements

This work was partially supported by the National Natural Science Foundation (No. 21961036), China Agriculture Research System (CARS-21), and Applied Basic Research Programs of Science and Technology Department of Yunnan Province (202101AT070041, 202002AA10007, 202102AE090042,

2019ZG0901). The study also was supported by the Key Laboratory of State Forestry Administration for Highly-Efficient Utilization of Forestry Biomass Resources in Southwest China (2019-KF05).

## Notes and references

- X. Xu, R. Ray, Y. Gu, H. J. Ploehn, L. Gearheart, K. Raker and W. A. Scrivens, *J. Am. Chem. Soc.*, 2004, **126**, 12736–12737.
- X. Zhang, M. Jiang, N. Niu, Z. Chen, S. Li, S. Liu and J. Li, *ChemSusChem*, 2018, **11**, 11–24.
- H. Tao, K. Yang, Z. Ma, J. Wan, Y. Zhang, Z. Kang and Z. Liu, *Small*, 2012, **8**, 281–290.
- L. Ai, Y. Yang, B. Wang, J. Chang, Z. Tang, B. Yang and S. Lu, *Sci. Bull.*, 2020, **66**, 839–856.
- J. Ding, L. Zhong, Q. Huang, Y. Guo, T. Miao, Y. Hu, J. Qian and S. Huang, *Carbon*, 2021, **177**, 160–170.
- Q. Huang, Y. Guo, D. Chen, L. Zhang, T. T. Li, Y. Hu, J. Qian and S. Huang, *Chem. Eng. J.*, 2021, **424**, 130336.
- X. Wang, A. Dong, Y. Hu, J. Qian and S. Huang, *Chem. Commun.*, 2020, **56**, 10809–10823.
- B. Sun, L. Duan, G. Peng, X. Li and A. Xu, *Bioresour. Technol.*, 2015, **192**, 253–256.
- Y. An, X. Lin, Z. Guo, Q. Yin, Y. Li, Y. Zheng, Z. Shi, W. Zhang and C. Liu, *Materials*, 2021, **14**, 4716.
- Z. Wang, B. Fu, S. Zou, B. Duan, C. Chang, B. Yang, X. Zhou and L. Zhang, *Nano Res.*, 2016, **9**, 214–223.
- L. Wang, W. Li, L. Yin, Y. Liu, H. Guo, J. Lai, Y. Han, G. Li, M. Li, J. Zhang, R. Vajtai, P. M. Ajayan and M. Wu, *Sci. Adv.*, 2020, **6**, eabb6772.
- Y. An, X. Lin, Y. Zhou, Y. Li, Y. Zheng, C. Wu, K. Xu, X. Chai and C. Liu, *RSC Adv.*, 2021, **11**, 26915–26919.
- P. K. Sarawat and M. L. Free, *Phys. Chem. Chem. Phys.*, 2015, **17**, 27642–27652.
- S. K. Bhunia, S. Nandi, R. Shikler and R. Jelinek, *Nanoscale*, 2016, **8**, 3400–3406.
- Y. Chen, M. Zheng, Y. Xiao, H. Dong, H. Zhang, J. Zhuang, H. Hu, B. Lei and Y. Liu, *Adv. Mater.*, 2016, **28**, 312–318.
- T. H. Kim, A. R. White, J. P. Sirdaarta, W. Ji, I. E. Cock, J. S. John, S. E. Boyd, C. L. Brown and Q. Li, *ACS Appl. Mater. Interfaces*, 2016, **8**, 33102–33111.
- G. Li, Y. Tian, Y. Zhao and J. Lin, *Chem. Soc. Rev.*, 2015, **44**, 8688–8713.
- E. F. Schubert and J. K. Kim, *Science*, 2005, **308**, 1274–1278.
- U. Kaufmann, M. Kunzer, K. Köhler, H. Obloh, W. Pletschen, P. Schlotter, J. Wagner, A. Ellens, W. Rossner and M. Kobusch, *Phys. Status Solidi A*, 2002, **192**, 246–253.
- Y. Zhang, P. Zhuo, H. Yin, Y. Fan, J. Zhang, X. Liu and Z. Chen, *ACS Appl. Mater. Interfaces*, 2019, **11**, 24395–24403.
- Q. Wang, Y. Gao, B. Wang, Y. Guo, U. Ahmad, Y. Wang, Y. Wang, S. Lu, H. Li and G. Zhou, *J. Mater. Chem. C*, 2020, **8**, 4343–4349.
- K. Jiang, S. Sun, L. Zhang, Y. Lu, A. Wu, C. Cai and H. Lin, *Angew. Chem.*, 2015, **127**, 5450–5453.
- C. D. Stachurski, S. M. Click, K. D. Wolfe, D. Dervishogullari, S. J. Rosenthal, G. K. Jennings and D. E. Cliffl, *Nanoscale Adv.*, 2020, **2**, 3375–3383.



- 24 A. Sharma, T. Gadly, A. Gupta, A. Ballal, S. K. Ghosh and M. Kumbhakar, *J. Phys. Chem. Lett.*, 2016, **7**, 3695–3702.
- 25 L. Tang, R. Ji, X. Li, G. Bai, C. P. Liu, J. Hao, J. Lin, H. Jiang, K. S. Teng, Z. Yang and S. P. Lau, *ACS Nano*, 2014, **8**, 6312–6320.
- 26 J. Peng, W. Gao, B. K. Gupta, Z. Liu, R. Romero-Aburto, L. Ge, L. Song, L. B. Alemany, X. Zhan, G. Gao, S. A. Vithayathil, B. A. Kaiparettu, A. A. Marti, T. Hayashi, J. Zhu and P. M. Ajayan, *Nano Lett.*, 2012, **12**, 844–849.
- 27 J. Zhou, Y. Yang and C. Y. Zhang, *Chem. Commun.*, 2013, **49**, 8605–8607.
- 28 B. B. Wang, Q. J. Cheng, L. H. Wang, K. Zheng and K. Ostrikov, *Carbon*, 2012, **50**, 3561–3571.
- 29 C. Wang, Z. Xu, H. Cheng, H. Lin, M. G. Humphrey and C. Zhang, *Carbon*, 2015, **82**, 87–95.
- 30 D. Qu, M. Zheng, L. Zhang, H. Zhao, Z. Xie, X. Jing, R. E. Haddad, H. Fan and Z. Sun, *Sci. Rep.*, 2014, **4**, 1–11.
- 31 H. J. Yoo and B. E. Kwak, *Phys. Chem. Chem. Phys.*, 2020, **22**, 20227–20237.
- 32 A. Dutta, S. T. Trolles-Cavalcante, A. Cleetus, V. Marks, A. Schechter, R. D. Webster and A. Borenstein, *Nanoscale Adv.*, 2021, **3**, 716–724.
- 33 Y. Chen, H. Lian, Y. Wei, X. He, Y. Chen, B. Wang, Q. Zeng and J. Lin, *Nanoscale*, 2018, **10**, 6734–6743.
- 34 M. Ge, X. Huang, J. Ni, Y. Han, C. Zhang, S. Li, J. Cao, J. Li, Z. Chen and S. Han, *Dyes Pigm.*, 2021, **185**, 108953.
- 35 S. J. Park, H. K. Yang and B. K. Moon, *Dyes Pigm.*, 2021, **186**, 109063.

